Global Journal of Environmental Science and Management
(GJESM)

Homepage: https://www.gjesm.net/

Characteristics and circulation of archipelagic waters with the three-dimensional hydrodynamic model approach

Suhaemi[1,2], D.G. Bengen[2], C.P.H. Simanjuntak[3], A.F. Koropitan[2]

[1] Department of Marine Sciences, Faculty of Fisheries and Marine Science, University of Papua, Manokwari 98314, Indonesia

[2] Department of Marine Sciences and Technology, Faculty of Fisheries and Marine Science, IPB University, Bogor 16680, Indonesia

[3] Department of Aquatic Resources Management, Faculty of Fisheries and Marine Science, IPB University, Bogor 16680, Indonesia

ARTICLE INFO

ABSTRACT

BACKGROUND AND OBJECTIVES: The Misool Islands are lined up regularly from west to east, the southern part of Raja Ampat Archipelago, Papua - Indonesia. The geomorphology is distinctive, and the coral reef substrate causes turbulence. Misool waters are located in the Papuan bird's head seascape, passed by Pacific water masses. The assessment status of Misool waters as a conservation area does not include hydrodynamic aspects in the decision processes. The present study is fundamental for determining and changing essential areas for conservation. The main objective of this study is to the pattern of hydrodynamic processes and investigate the features of the water mass in the Misool waters.

METHODS: An acoustic doppler current profiler was deployed to measure currents every 15 minutes for ten water column layers. Investigation of waters characteristics was using Conductivity-Temperature-Depth equipment. A three-dimensional computational model was performed using MIKE3.

FINDINGS: The water mass around the Misool Islands are more influenced by the local oceanographic processes than the water masses from the Pacific Ocean. The study site is characterized by the mixed tide, prevalence to semi-diurnal based on observational tidal data. Wind and baroclinic properties generate non-significant currents, resulting in low horizontal and vertical stratification. Intensification of tidal currents occurs along the shallow part in northeastern and part of the channel between Misool Islands and the mainland of Papua.

CONCLUSION: The interaction of barotropic tides, geomorphology, and coral reef triggers the unstratified water mass. Strong currents and turbulence on the northeast side produce homogeneous waters. The water mass in Misool waters is originated from the local dynamic.

NUMBER OF REFERENCES
37

NUMBER OF FIGURES
10

NUMBER OF TABLES
1

*Corresponding Author:
Email: s.manaf@unipa.ac.id
Phone: 0813 4487 9586
ORCID: 0000-0003-4585-2277

Note: Discussion period for this manuscript open until January 1, 2023 on GJESM website at the "Show Article".

INTRODUCTION

The study of hydrodynamics, especially in coastal areas, is an important thing that needs to be done. Hydrodynamics is one of the water control systems that have implications for the distribution of marine life: transport of fish eggs and larvae (George *et al.*, 2013). It makes the hydrodynamics of the waters play a role in the sustainability of aquatic biodiversity. Monsoonal wind and density are driving forces for the hydrodynamics in the coastal area. In particular, coastal areas, tidal currents regulate material transport and biological processes and control the intensification of materials in the waters (Koropitan *et al.*, 2006). The current patterns greatly determine water quality, oxygen distribution, temperature, salinity, nutrient supply, primary productivity (Porter *et al.*, 2018). Tides and currents are significant for coastal development planning, management, conservation, fishing, and coastal mitigation. Understanding the hydrodynamic aspects of the waters requires a long and expensive field study and an applicable completion method. The best solution that can be done is through a three-dimensional modeling approach as a prototype of the natural and factual conditions. This approach has been carried out in several other areas, including Mayalibit Bay, Raja Ampat-Indonesia (Budiman *et al.*, 2014), Tomori Bay, North Morowali-Indonesia (Sabhan *et al.*, 2021), the Malacca Strait-Indonesia (Haditiar *et al.*, 2020), the West Coast of Badung Regency, Bali-Indonesia (Adhibusana *et al.*, 2016), Benoa Bay-Indonesia (Hendrawan *et al.*, 2005), and Ambon Bay (Noya *et al.*, 2016; Noya *et al.*, 2021). The modeling approach can be used in various water conditions, including archipelagic waters. One of the archipelagic areas with high urgency to study its hydrodynamics in Misool Islands. Misool Islands are the largest marine protected area with the highest biodiversity, located in the Raja Ampat Islands, Indonesia. Misool Islands are characterized by zonal-lined coral reef substrates and varying bathymetry (1 to 500 m). The combination of the original characteristics of the islands and the tidal dynamics produces variations in circulation (Zhang *et al.*, 2018). These interactions generate internal waves and stimulate mixing (Sabhan *et al.*, 2019). The shape of the waters of Misool Islands is semi-enclosed and resembles a channel, affecting tidal wave propagation (Ferrarin *et al.*, 2018) and sensitivity to bathymetry (Pringle *et al.*, 2018). Several studies that have been conducted on Misool Islands are still limited to the fisheries aspect, namely capture fisheries management (Sala, 2018), the ecological status of fish in Misool marine conservation (Sala *et al.*, 2020), observations of the Misool marine lake ecosystem (Purba, 2020; Sawairnathan and Halimoon, 2017), monitoring grouper spawning areas. Studies that underlie these aspects, including hydrodynamics, have never been carried out. Position of the Misool waters in the Papuan bird's head seascape network is passed by the Pacific water masses to the Indian Ocean. What is the influence of the Pacific water masses in the Misool Islands? The geographical position of the Misool waters, complex geomorphology, and coral reef substrates create a unique circulation pattern, and this statement needs to be proven. What is the impact of complex geomorphology and coral reef substrate on flow patterns in the waters of the Misool Islands, West Papua? The present study aims to examine the hydrodynamics processes of the Misool Islands. The objectives of this study are to investigate the characteristics of waters masses and to analyze the impact of complex geomorphology and coral reef substrate on flow patterns in Misool waters. This study has been carried out in Misool waters during 11 - 14 May 2019 for water mass measurement and during 9 - 21 January 2020 for ocean current measurement.

MATERIALS AND METHODS

Area study

Misool Islands are located in the Raja Ampat Archipelago, West Papua Province, Indonesia. The islands have an area of 2,034 square kilometers with the highest elevation of 535 m above sea level. This island is located on the bird's head of West Papua and is directly adjacent to the Seram Sea on the south and west sides and the Halmahera Sea on the west. The waters of Misool Islands have shallow bathymetry on the east and south sides, while the west and southwest sides are deep. The water depth ranges from 1 to 500 m. Misool Islands are one of the world's coral triangles with high biodiversity and are the largest conservation area in Raja Ampat (346,189 ha). Besides coral reefs, Misool Islands' biodiversity includes turtles, manta rays, saltwater crocodiles, seagrass beds, and mangroves. Misool Islands waters are also one of the transmigration routes of whales and octopuses.
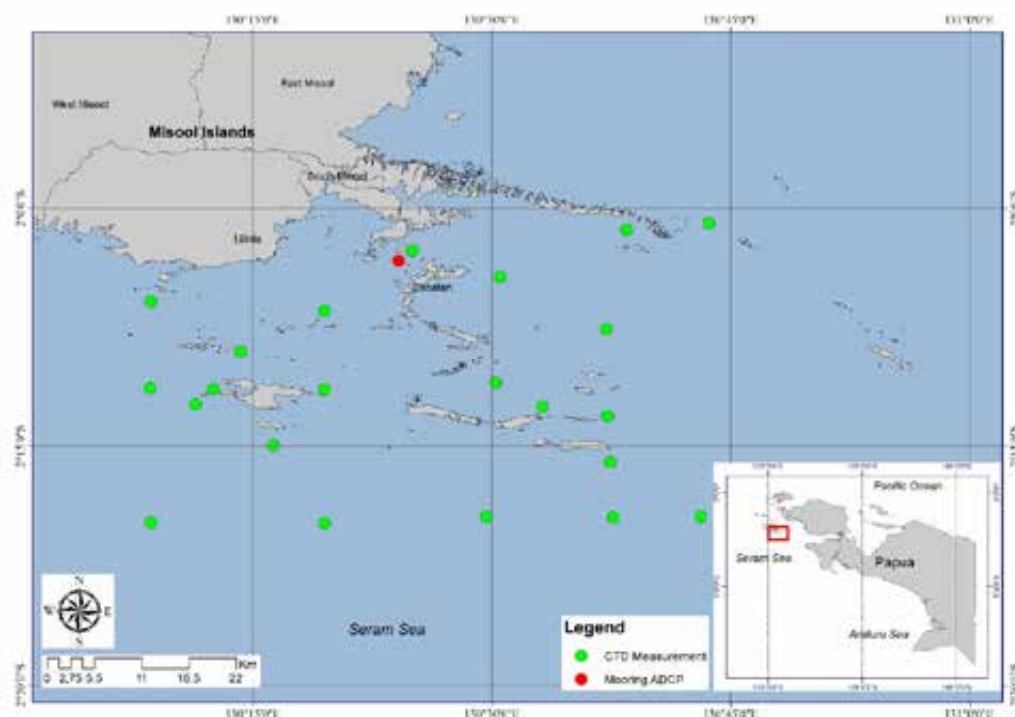
Fig. 1: Geographic location of the study area and station sampling in Misool, West Papua, Indonesia

Field sampling

Tidal forces and geomorphology were controlling current patterns in the Misool waters. Identification of the Misool waters characteristics (depth, temperature, conductivity, density) vertically and horizontally was carried out using Conductivity-Temperature-Depth (CTD) equipment at 22 stations during 11 - 14 May 2019 (Fig. 1). The CTD was deployed slowly at each station until closed to the bottom water (monitored directly via the control unit on the boat). The bathymetry (interval 10 m - 100 m) around Misool Islands was recorded using Single-Beam Echosounder G-2108. The echosounder was installed on the boat and recorded on a pre-set path. The pre-set path is perpendicular to the shoreline and concentrated on coastal areas and small islands. To avoid bias, the boat speed is adjusted around 2.5 m/s - 3.0 m/s (Koropitan *et al.,* 2021). The current was observed 13 days (9 - 21 January 2020) by employing the Acoustic Doppler Current Profiler (ADCP) SonTek Argonaut-XR (accuracy 0.5 cm/s). The ADCP was deployed at 27 m depth, equipped with buoys and anchors, and recorded every 15 minutes in 10 water column layers.

Hydrodynamic modeling

The ecological processes of Misool waters were approached using the three-dimensional (3D) numerical model by using MIKE3. Numerical solutions are based on the Navier-Stokes equation, the Boussinesq approximation, and hydrostatic pressure. The turbulent waters conditions were determined using the eddy viscosity concept. Turbulence parameters using the standard k-ε (Canuto *et al.,* 2001) and vertical eddy viscosity using the concept of Smagorinsky (1963).

The continuity is used as Eq. 1.

$$\frac{\partial u}{\partial x} + \frac{\partial v}{\partial y} + \frac{\partial w}{\partial z} = S \tag{1}$$

The horizontal momentum for the x-component is used as Eq. 2.

$$\frac{\partial u}{\partial t} + \frac{\partial u^2}{\partial x} + \frac{\partial vu}{\partial y} + \frac{\partial wu}{\partial z} = fv - g\frac{\partial \eta}{\partial x} - \frac{1}{\rho_0}\frac{\partial P_a}{\partial x} - \frac{g}{\rho_0}\int_z^\eta \frac{\partial \rho}{\partial x}dz - \frac{1}{\rho_0 h}\left(\frac{\partial S_{xx}}{\partial x} + \frac{\partial S_{xy}}{\partial y}\right) + F_u + \frac{\partial}{\partial z}\left(v_t\frac{\partial u}{\partial z}\right) + u_s S \tag{2}$$

The horizontal momentum for the y-component is used as Eq. 3.

$$\frac{\partial v}{\partial t} + \frac{\partial v^2}{\partial y} + \frac{\partial uv}{\partial x} + \frac{\partial wv}{\partial z} = fu - g\frac{\partial \eta}{\partial y} - \frac{1}{\rho_0}\frac{\partial P_a}{\partial y} -$$
$$\frac{g}{\rho_0}\int_z^\eta \frac{\partial \rho}{\partial y}dz - \frac{1}{\rho_0 h}\left(\frac{\partial S_{yx}}{\partial x} + \frac{\partial S_{yy}}{\partial y}\right) + F_v +$$
$$\frac{\partial}{\partial z}\left(v_t\frac{\partial v}{\partial z}\right) + v_s S \qquad (3)$$

Model set-up, initial conditions, and boundary conditions

The Misool waters system is designed in a flexible mesh based on sigma coordinates (10 layers). The model domain is set to 7000 Km^2, 100 Km in zonal direction, and 70 Km in the meridional direction. The flexible mesh is also made in detail in the east-south Misool (conservation area). It also accommodates the simulation's tides, wind, salinity, and temperature. The time step was 30 seconds, 3D turbulent variables used k-epsilon, and vertical viscosity factors followed the Smagorisky formula based on an earlier study (Pradhan *et al.,* 2020). Based on the pre-test, it was found that the best viscosity and vertical diffusivity coefficient in Missol waters are 1.8x10^{-6} m^2/s, higher than the previous study, which only 10^{-7} m^2/s (Seiler *et al.,* 2020). The roughness sensitivity (Manning number) and horizontal turbulent viscosity are 0.02 - 0.05 and 1 m^2/s - 10 m^2/s. At the initial condition (t = 0), the waters conditions were assumed constant in all computational domains, and without vertical and horizontal disturbances (u = v = η = 0). Temperature and salinity are initialized vertically at the open boundary (Sorourian *et al.,* 2020). At the open boundary, the current is generated from the tide, temperature (29°C), salinity (33 PSU), and wind. The Misool sea level elevation data originated from the tide model in the toolbox of the Danish Hydraulic Institute (DHI). The temperature and salinity are derived from CTD measurements. The wind obtained from the European center for medium-range weather forecasts (ECMWF) reanalysis (0.125° by 0.125° resolution) in two years (2019 - 2020).

RESULTS AND DISCUSSION
The current profile of Misool waters

The ADCP data showed that the current is varied among layers. The strongest current (maximum 0.86 m/s, an average of 0.26 m/s) was recorded near-surface layers. The weakest (maximum 0.36 m/s, an average of 0.10 m/s) was near the bottom. This study found that the currents vector is not in line with depth (Fig. 2). This weakening is due to the non-linear impact of weakening winds on depth and increasing base resistance (Lee dan Beardsley, 1999). Misool waters with coral reef substrate have a high bottom resistance and reduce the current velocity. Layer 1 to 4 the current variation is homogeneous, a maximum of 0.36 m/s - 0.39 m/s, a minimum 0.001 m/s - 0.003 m/s and an average 0.01 m/s - 0.14 m/s. Layer 5 and layer 6 maximum current is 0.44 m/s and 0.59 m/s, an average 0.17 and 0.20 m/s and a minimum 0.004 m/s. Layer 7 to 10 maximum current 0.73 m/s, 0.83 m/s, 0.86 m/s, and minimum 0.006 m/s. Hadikusumah (2010) finds a similar pattern. The Misool waters current varied 0.002 m/s - 0.74 m/s. The current direction shows an alternating regularity pattern, describing Misool waters as the dominant tidal current. The main current direction to the northeast and southwest align with the tidal propagation. The current vector in layers 1 to 3 is dominant to the southwest (200° - 250°), with 22.68% - 24.37% frequency. Layers 4 to 9 are dominant to the northeast (20° - 70°) with a frequency of 32.05% - 35.24%, and layer ten dominant current 34.11% moving to the southwest (200° - 250°). The dominant current towards the northeast and southwest ensures that the dominant force of the Misool waters is tidal. At high tide, the current enters the Misool waters to the northeast and at low tide to the southwest. The waters of Misool are open on the west and south sides, bordering the Seram Sea. The Mainland of Papua connects the east side, contributing to the arrangement of the alternating flow pattern. The current circulation formed is the resultant of all the constituents of the current force. The separation of the tidal currents and residual currents indicates that the tidal currents are dominant. The maximum current was 0.64 m/s, the maximum residual current was 0.22 m/s. The non-linear effect is seen in the residual current with an irregular direction. Tidal currents create a regular pattern; at high tide, it moves to the northeast and at low tide to the southwest. Tidal currents to the northeast (20° - 70°) with a frequency of 42.70%, a maximum speed of 0.32 m/s, and an average of 0.15 m/s. The southwestward current (200° - 250°) has a frequency of 21.35%, a maximum of 0.31 m/s, and an average of 0.14 m/s. The percentage of tidal currents during the flood was more dominant
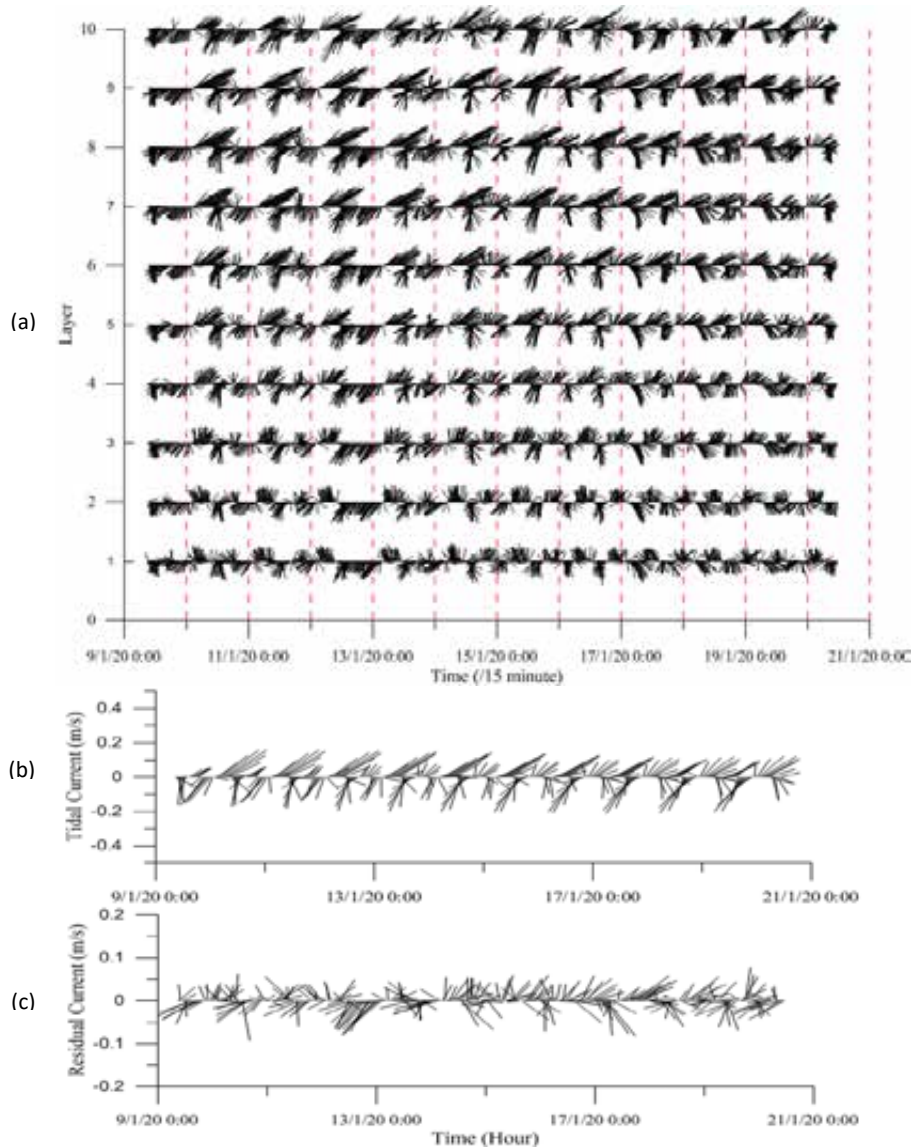
Fig. 2: Water current profile at ten layers (a); the separation of the tidal current (b) and residual current (c) components averaged to depth.

than low tide. Misool Islands are characterized by the mixed tide: semi-diurnal tides with two high tides and one low tide. The residual current flow is random, to the northeast, southwest, northwest, north, and southeast, with frequencies of 26.22%, 20.97%, 11.61%, 10.49%, and other 9.74% spread out in various directions with a small percentage. Unidirectional with the westerly monsoon that blows over the Misool waters in January, the dominant residual current spreads to the northeast. There is a positive relationship between the westerly monsoon and residual current, the westerly monsoon from the southwest, and the dominant residual current to the northeast. The progressive vector of the residual current to the northeast has a maximum speed of 0.18 m/s, with an average of 0.08 m/s. The residual current to the southwest has a maximum speed of 0.22 m/s and an average of 0.11 m/s. The velocity of the residual current that moves to the southwest is greater than the northeast direction.
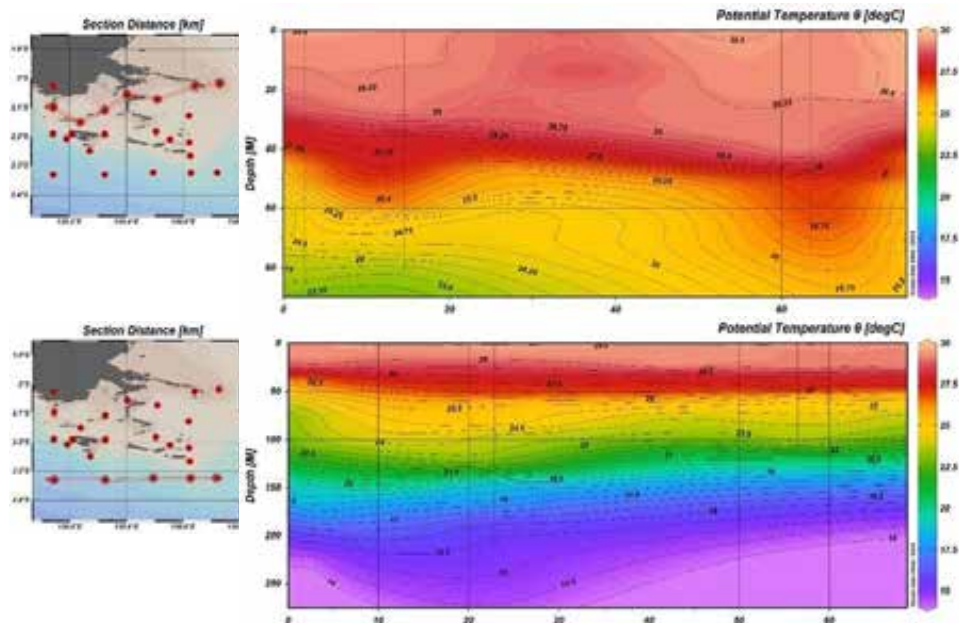
Fig. 3: The observation of spatial vertical temperature of Misool waters

Temperature and salinity of Misool waters

The characteristics of the Misool waters (temperature, salinity, density) are based on CTD recording data. This study found that the vertical water's temperature ranged from 28.9°C to 29.7°C, with an average of 29.5°C (Fig. 3). This temperature is characteristic of warm tropical waters. These findings were confirmed by a previous study that found the tropical waters have a surface temperature greater than 28°C and a range of 28°C - 30°C, and temperature variations increase towards the ocean (Ilahude and Gordon, 1996). Fig. 3 shows the vertical temperature profile from 0 to 350 m (CTD depth limit). The southern CTD station in Misool waters found that the vertical temperature varied between 14°C - 29.7°C, indicating mixed and thermocline layers in the water column. The other areas (east, northeast, and southeast) show the homogenous layers in the water column (Fig. 3). The homogenous layer is due to the shallow waters in those areas, combined with the strong current, which is the main energy for the mixing force. The maximum mixed layer depth (MLD) on Misool water was 100 m and characterized by homogeneous temperature (25.5°C - 29.5°C). The MLD shows different depths at several observation stations but has a similar pattern. The local thermocline layer in tropical waters is

characterized by extreme temperature changes (over to 20°C) (Hutabarat *et al.,* 2018) and changes in the density of 0.15 kg/m³ for each added 10 m depth (Thomson and Emery, 2014). This study found a declining temperature of 20.0°C - 21.5°C at a depth of 100 m, the thickness of the thermocline layer reaches 100 m, and the boundary between the lower thermocline and the inner layer is at a depth of > 250 m. The vertical salinity distribution for each station is invariant between stations and in line with the depth increase (Fig. 4). Depth 0 m - 100 m salinity is homogeneous, increasing at deeper depths. A depth of 100 m - 200 m indicates a halocline layer with significant salinity changes and a salinity core found at a depth of 150 m (34.25 PSU). The salinity profile is homogeneous on the northeast of the Misool waters, ranging from 32.45 PSU to 33.45 PSU. The surface salinity showed homogeneity in the range of 32.50 PSU. The vertical profile has an increasing salinity variation with depth 32.00 PSU - 34.25 PSU. The horizontal profile of salinity has a similar pattern to the temperature. The maximum salinity of 32.50 PSU was found at the Parongket Island station. The minimum salinity was found in the coastal area near the mainland of Papua. Low salinity is found at the mainland boundary due to freshwater intrusion from the Misool Islands and the west side of the river
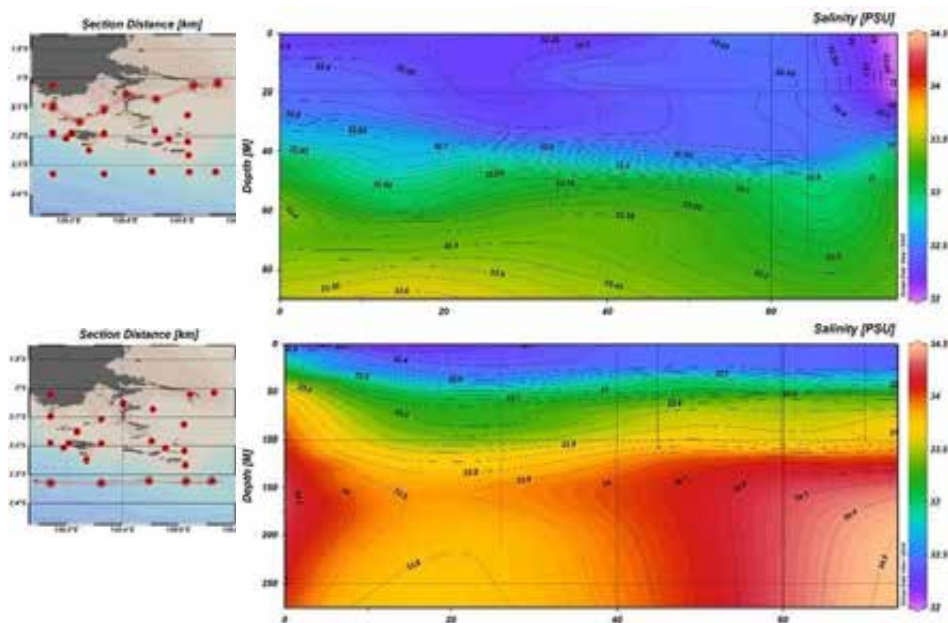
Fig. 4: The observation of spatial vertical salinity of Misool waters

discharge from the Kaimana and Bintuni Islands. Fig. 4 shows the vertical salinity distribution in the 0 m - 50 m layer of 32.15 PSU - 32.50 PSU. The salinity increases of 33.10 PSU - 33.90 PSU at a depth of 50 m - 100 m, and the maximum salinity is found at a depth of 150 m, which is 34.25 PSU. The salinity dropped to 33.85 PSU again at a depth of 200 m to the CTD depth limit. This pattern only occurs on the west and southwest sides. The east, northeast, and southeast are homogeneous vertically. In the southwest and south, at a depth of 150 m, the observation station between latitude -2.3° and longitude 130.2° - 130.4° forms a high salinity front. It is possibly due to the high salinity spooky seawater mass in the south and southwest touching with the origin water mass of Misool. As a reference, it is known that the waters off the coast of the Seram Sea have a salinity > 34.5 PSU, which is advanced than the salinity of the Misool waters < 33.5 PSU.

Characteristics of the Misool water mass

The Misool water mass description is illustrated in the T_{pot}-S diagram (Fig 5). This diagram found that the salinity increases (maximum of 34.25 PSU) from the surface to 200 m depth and then decreases at a depth of more than 200 m. It is shown by the sigma-t value, which drops at a depth of more than 250 m. At

a depth of 150 m - 200 m, salinity is stable at 33.75 PSU -34.00 PSU and a sigma-t value of 24.5 kg/m³. There is no similarity between the Misool water mass and the North and South Pacific water mass based on the T_{pot}-S diagram. It indicates that the water mass in our study area originates from Misool waters. The Misool waters are in a Papuan bird's head seascape network, where Pacific water masses cross the seas as Indonesian Throughflow (ITF). Halmahera eddy deflects Pacific water masses that flow through the eastern route. The rest is pushed through the Maluku Sea and the Seram Sea, entering the Banda Sea and exiting Indonesian waters through the Flores Sea and the Timor Sea. The water mass of the ITF is a mass of deep water that flows at a depth of more than 100 m, while the waters of the southeast Misool are shallow. This finding aligns with Radjawane and Hadipoetranto (2014), which stated that the ITF originating from the North Pacific and South Pacific via the eastern route does not flow directly to the Misool Islands waters. Hadikusumah (2010) explained that the Misool waters in the mixed layer to a depth of < 100 m found a temperature range between 29.26°C - 27.00°C and salinity between 33.90 PSU - 34.21 PSU. These conditions exhibit characteristics analogous to those obtained in this study. The characteristics of the waters (Fig. 5) show that the mixed layer is found
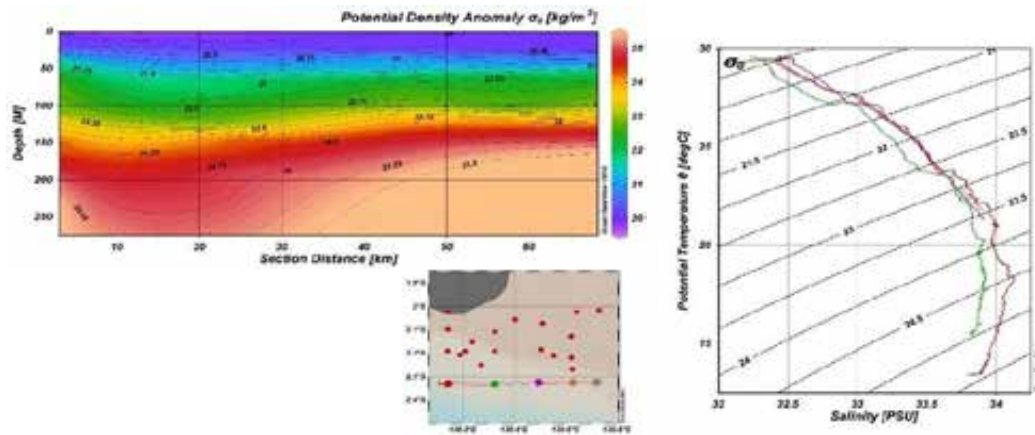
Fig. 5: The observation of vertical density potential and T_{pot}-S diagram of Misool waters

Table 1: Comparison of tidal current (ellipse constituents) between model results and observation

Layer	Tidal constituents	Delta major ellipse (cm/s)	Delta minor ellipse (cm/s)	Delta inclination (degree from the east)	Delta phase (°GMT)
1_bottom	K1	8.22	1.58	0.71	128.83
4_column	K1	3.03	0.25	25.34	150.17
7_column	K1	1.24	0.88	22.30	145.16
10_surface	K1	6.79	0.94	3.78	145.94
1_bottom	M2	2.65	1.58	26.83	12.68
4_column	M2	1.24	3.79	7.02	15.14
7_column	M2	2.28	2.08	13.54	0.28
10_surface	M2	4.32	3.43	11.96	23.13
1_bottom	O1	2.74	3.39	36.09	77.60
4_column	O1	0.86	0.62	5.77	79.62
7_column	O1	1.99	0.94	3.59	81.30
10_surface	O1	1.52	0.77	8.19	76.09
1_bottom	S2	0.32	0.92	7.35	4.54
4_column	S2	0.82	0.19	8.88	4.68
7_column	S2	0.21	0.03	19.41	16.99
10_surface	S2	3.94	0.69	24.86	8.68

at a depth of 50 m with a temperature of 27.5°C - 29.0°C and salinity of 32.5 PSU - 32.8 PSU; at a depth of 50 m - 100 m, the temperature decreases to 24.5°C - 25.5°C and salinity of 33.5 PSU - 33.6 PSU. It is found that significant temperature changes of 22°C - 17.5°C at a depth of 125 m - 225 m. T_{pot}-S diagram shows red and green lines, indicating different salinity characteristics, with the green line reaching a maximum salinity of 33.8 PSU found at a depth of 150 m - 200 m.

Hydrodynamic modeling of Misool waters
Model verification

The model results and field observations were

verified to be very good and coherent, showing the same regularity pattern. Table 1 shows the deviation of the four major constituents in the four water layers. The difference in values for the major ellipse is 0.21 cm/s - 8 cm/s and the minor ellipse is 0.03 cm/s - 3.79 cm/s. The model results and observations also show a small phase difference value. The smallest difference in the main tidal ellipses of the main luni-solar diurnal (K1), main lunar semi-diurnal (M2), main lunar diurnal (O1) and main solar semi-diurnal (S2) is 1.2 cm/s, 1.2 cm/s, 0.86 cm/s and 0.21 cm/s. The difference in the maximum inclination value of 36.09° is much lower than required (45°) (Koropitan *et al.,* 2021). The model applied to the Misool waters gives excellent results in describing the natural characteristics.

Fig. 6 shows the tidal current ellipse of the diurnal constituents (K1, O1) and the semi-diurnal constituents (S2, M2). An acceptable current ellipse will show a pattern of model results in line with the observations. The elliptical vertical tidal current structure has a low amplitude to depth for K1, O1, M2, and S2 constituents. The elliptical vertical tidal current structure has a low amplitude to depth for K1, O1, M2, and S2 constituents. The ellipses of major and minor axes, the direction of rotation, and constituent phases K1 and M2 rotate to the right. On

the layer near the bottom, the rotation changes to the left. It is could be due to stratification (Izquierdo dan Mikolajewicz, 2019). In all water column layers, the elliptical rotation of constituents O1 and S2 is consistent to the right. Based on the geomorphology, the tidal elliptical constituents K1, O1, S2, and M2 are oriented parallel to the central axis on Misool Islands. Tidal currents move gradually from south to southwest. The maximum tidal current K1 was recorded near the surface. The principal axis velocity (30 cm/s) is obtained near the surface and decreases as depth increases. The layer near the bottom has a speed of 5 cm/s. The tidal current ellipse of the constituents O1, M2, and S2 shows similar to K1 but with different values. The maximum velocities of the tidal currents O1, M2, and S2 occur in the layer near the surface at speeds of 15 cm/s, 50 cm/s, and 10 cm/s. Verification of the modeling results still shows differences in velocity, orientation, and phase for each constituent. The difference is thought to be due to the non-linear factor value, which is not absolute yet but is close to absolute. The Misool waters have non-uniform basic substrate characteristics in all model domains. The value of the necessary roughness is represented by the constant Smagorinsky value and causes errors in the modeling computation. These
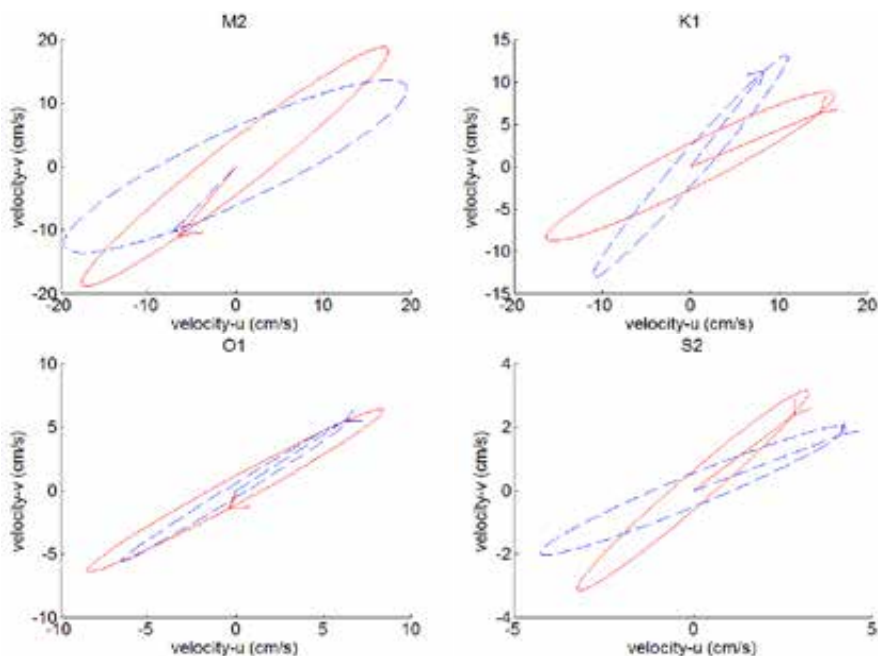

Fig. 6: Comparison between field observations (red) and model (blue) results for M2, O1, K1, S2 tidal currents

errors can be minimized by using a high-resolution domain grid and nesting in a single execution.

Simulation of tidal current patterns

Tidal forces dominate the main generator of the Misool water circulation. The main tidal constituents of Misool waters are M2, S2, K1, and O1. The ellipse of the Misool waters spatially shows variations in the range of 1.5 to 65 cm/s. Strong currents are noticed between the mainland and surrounding the islands in the strait system, and slow currents near the shore. Misool waters are the waters around the islands with a flow pattern following the topographic contours. The inflow and outflow follow flood and ebb conditions. The amplitude and propagation of tides vary. Significant velocities are seen at the land boundary inlet and narrow passages. This condition is in line with what was found by Sorourian *et al.* (2020); Sabhan *et al.* (2021). Misool with archipelagic characteristics, random bathymetry, and coral reef substrates influence tidal dynamics. Tides and their propagation are controlled by geomorphology and irregular coastlines (Ivanov *et al.,* 2020). These conditions stimulated the mixing of the water column. The interaction of barotropic tides with geomorphology triggers well mixed. This pattern can be seen on the southwestern and northeastern sides. Homogeneous waters with strong currents occur on the shallow northeast side. On the southwest side, stratification is visible. Tidal and topography interactions modulate diurnal and semi-diurnal tidal ellipses (Quaresma dan Pichon, 2013). Topographic interactions affect the tidal amplitude and induce strong currents. The coral bathymetry provides greater basic friction (Colberg *et al.*, 2020), the decay of energy by friction results in an amplitude decay (Cook *et al.,* 2019). Topographic characteristics make the tidal propagation pattern at flood and ebb. Complex topography in Misool Islands produces the tidal propagation pattern during flood and ebb tides. The mainland of Papua deflects the tidal propagation on the east and northeast sides; in the west, the tidal propagation is held back by Halmahera Island. Strong currents in the Halmahera Strait and the Maluku Islands in the south a role in pushing the water mass to the southeast, leaving the Misool waters. The magnitude of the tidal constituent varies in its propagation, and this is due to water geometry
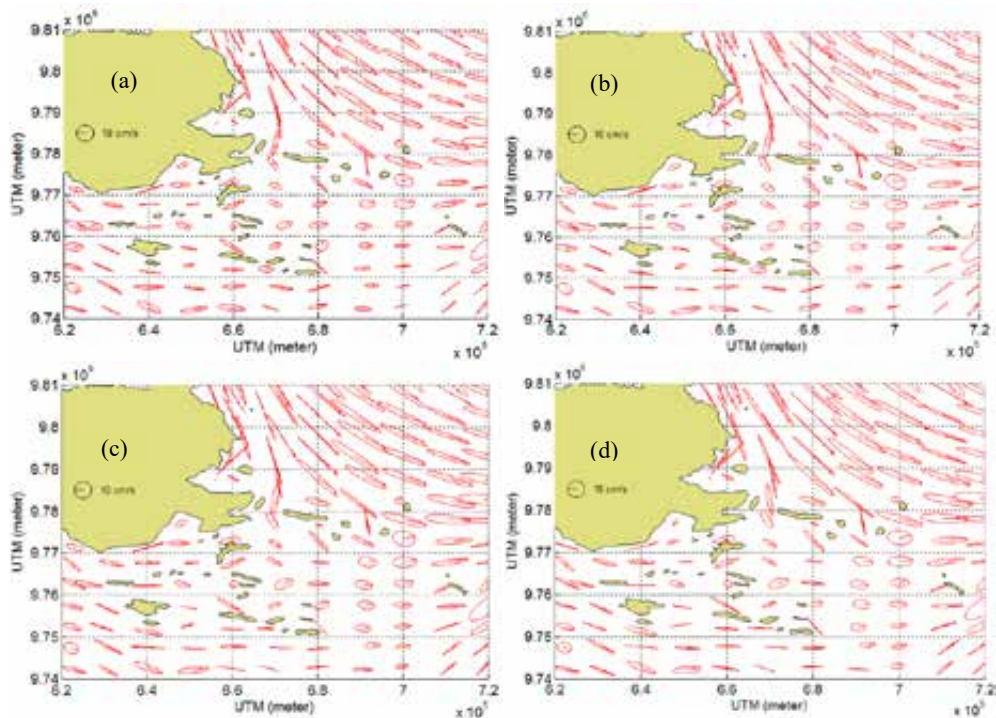

Fig. 7: The calculated K1 tidal current in layer-1 near the bottom (a), layer-4 of water column (b), layer-7 of water column (c), and layer-10 at the surface water (d)
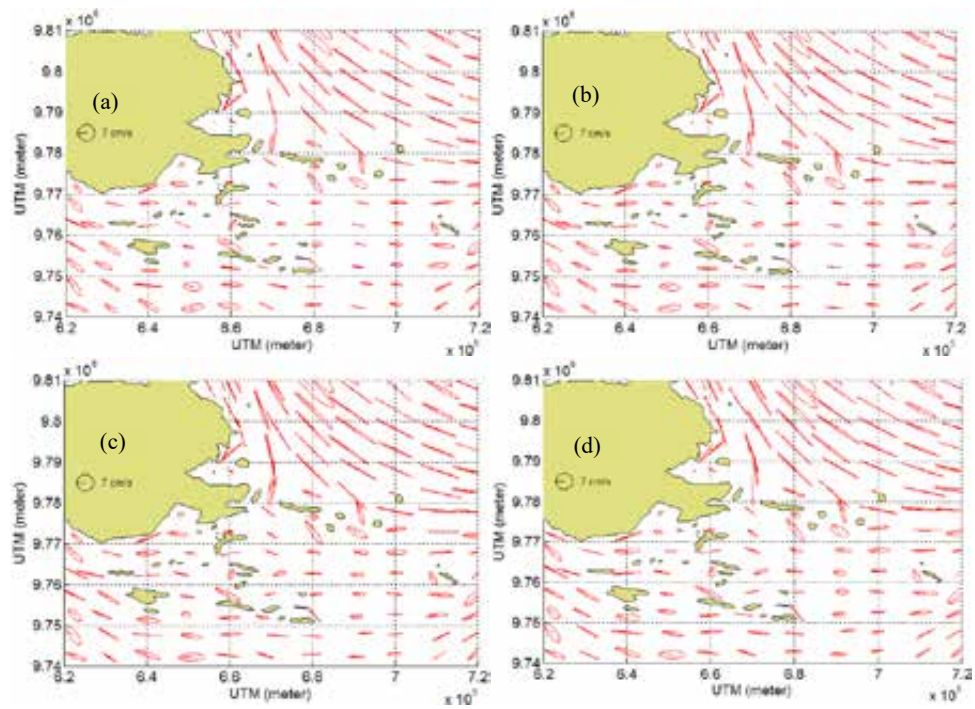
Fig. 8: The calculated O1 tidal current in layer-1 near the bottom (a), layer-4 of water column (b), layer-7 of water column (c), and layer-10 at the surface water (d)
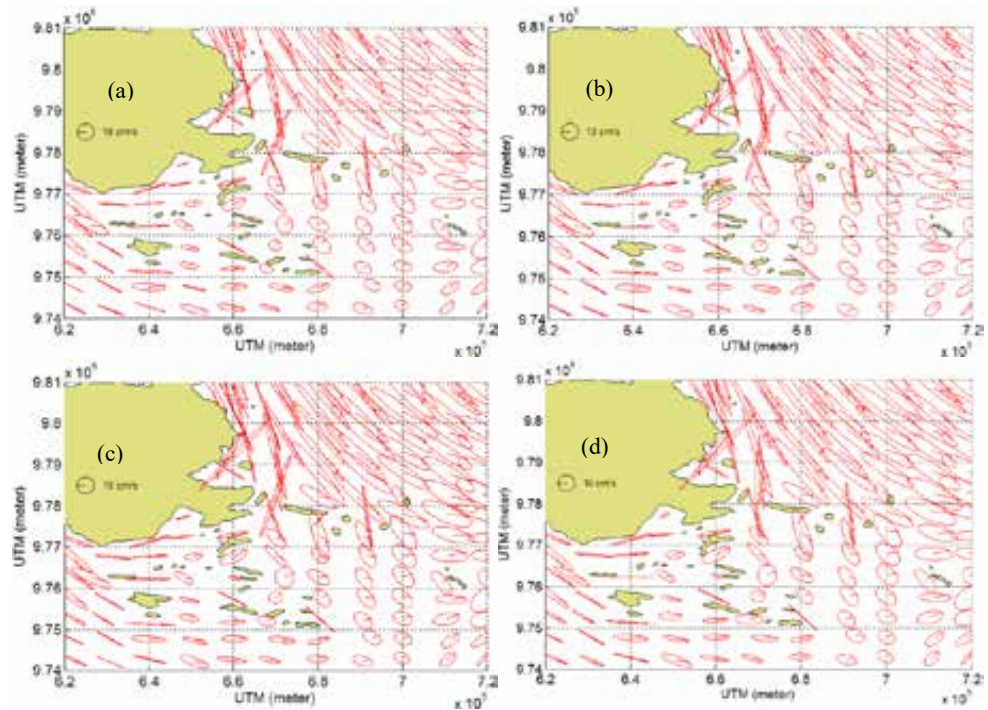
Fig. 9: The calculated M2 tidal current in layer-1 near the bottom (a), layer-4 of water column (b), layer-7 of water column, and layer-10 at the surface water (d)

factors (Rijn, 2011). Tidal deformation of the waters is increased by lateral constriction (Pradhan *et al.*, 2020). The isoline amplitude follows the depth contour. The signal of the semi-diurnal constituent is more robust in the ocean than in the coastal area. The tidal propagation of M2 and S2 constituents, from southeast to northwest, has a phase difference of 40°. Tidal current velocity for all diurnal constituents (K1, O1) and semi-diurnal constituents (M2, S2) is strong along the shallow part in northeastern, and also part of channel between Misool Islands and the mainland. The current velocity constituent of K1 has a maximum of 50 cm/s, and an average of 20 cm/s. Vertically the velocity shows variation. The maximum velocity occured in the layer near the surface reaches 50 cm/s, an average of 20 cm/s, and in the layer near the bottom, the top speed is 40 cm/s, an average of 17 cm/s (Fig. 7). The O1 tidal currents show a similar pattern to K1 tidal currents. Large velocity occurs at the strait and the continental shelf

boundary with reduced velocity near the bottom (Fig. 8). The O1 constituent has a maximum velocity of 28 cm/s with an average of 11 cm/s in the near-surface layer. The near-bottom layer has a maximum of 20 cm/s with an average of 9 cm/s. Figs. 9 and 10 show that the semi-diurnal tidal currents have a similar pattern with the diurnal tidal currents with different velocities. The M2 surface tidal currents have a maximum of 65 cm/s and an average of 29 cm/s. The S2 surface tidal currents have a maximum of 20 cm/s and an average of 10 cm/s. The tidal currents in Misool waters show a strong influence by the semi-diurnal tide, particularly M2. The tidal currents vary in vertical profile with maximum velocity in the layer near-surface and decrease near the bottom layer. Strong velocities are also formed along the boundary area for all tidal constituents. In the case of Misool waters, the vertical stratification is less, resulting in a small effect on inducing currents due to stratification.
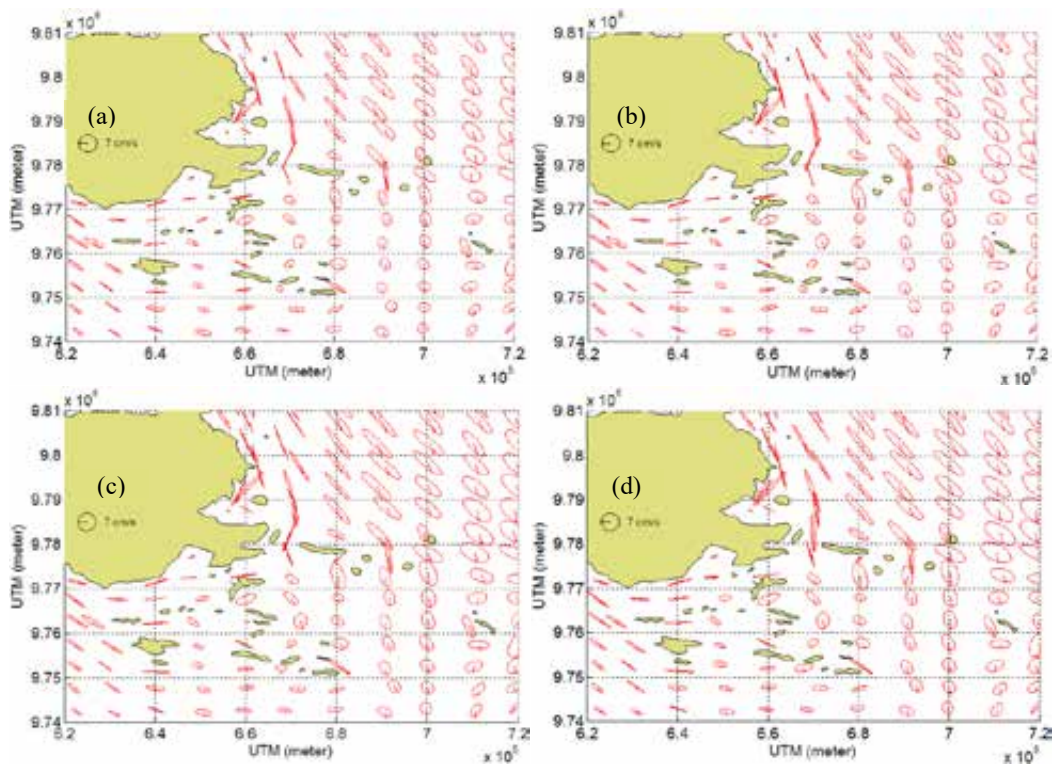

Fig. 10: The calculated S2 tidal current in layer-1 near bottom (a), layer-4 of water column (b), layer-7 of water column (c), and layer-10 at the surface water (d)

CONCLUSION

This study successfully investigates the characteristic water mass and hydrodynamic processes of Misool waters. The depiction of the water mass characteristics of Misool waters, as the Tpot-S diagram, does not show similarities to the water masses of the north and south Pacific water masses. It is characterized as origin water masses from the Misool waters. The water column is stable until the CTD depth limit; the surface layer to a depth of 200 m increases with a maximum salinity of 34.25 PSU, salinity decreases at a depth of 200 m to the CTD depth limit. The Misool waters are in a Papuan bird's head seascape network, and the Pacific water mass passes these waters as the ITF. Still, the Pacific water mass has no impact on the Misool water masses. The Halmahera eddy deflects the Pacific water masses that pass through the eastern route, and the rest is pushed through the Maluku and Seram Seas. The water masses from the Pacific Ocean flow mainly at a depth of more than 100 m, while the southeast Misool waters are shallow. Based on modeling and observations data, it was found that the tides are the main force that generates water circulation on the study site. These characters are represented from ADCP recording (maximum tidal current 65 cm/s, and maximum residual current 25 cm/s). The modeling showed that 50% of the tidal current formation components are semi-diurnal (M2) components, followed by K1, O1, and S2 components. The currents generation by wind and baroclinic properties showed the non-significant value and produced small horizontally and vertically stratification. It indicates that it has minimal effect in inducing current circulation. The tidal component amplitudes are rectified at the continental margin for all diurnal (K1, O1) and semi-diurnal (M2, S2) components. The tidal component vertically varies with the strongest magnitude in the near-surface layer. The Misool Islands are characterized by mixed tidal, prevalence to semi-diurnal. It is confirmed by the maximum speed of each component, which is 67 cm/s, 50 cm/s, 28 cm/s, and 20 cm/s for M2, K1, O1, and S2. Based on echosounder data, the bathymetry of Misool waters is varied between 1 m to 500 m depth. It also noted that the seabed forms an extreme slope around the coral reef islands (100 m - 200 m from the coastline). The island's geomorphology and coral reef substrates impact the rectification of tidal currents. Shallow bathymetry is on the eastern and northeastern sides of the islands. It creates the decay of tidal energy at high tide that propagates to the east and northeast. Tidal energy is strengthened during propagation towards the west, southwest, and southeast. According to pre-test, the 3D modeling domain for coral reef substrates obtained the best origin constant values, the coefficient of viscosity, and vertical diffusivity of 1.8×10^{-6} m^2/s. The hydrodynamic model was first applied to Misool waters. The present study is limited to tidal current modeling, and temperature and salinity to describe the Misool waters origin characteristics. This study needs to be re-examined for a more extended period and detailed modeling with monsoonal wind and baroclinic effects. The status of Misool waters as a conservation area does not include hydrodynamic aspects in the decision substance. This study is fundamental as a guide for determining and changing essential areas for conservation, defining the boundaries of fishing areas in the Spawning aggregation site (SPAGs) and the distribution area of fish larvae. The future research plan is modeling the distribution of multi-species coral reef fish. Hydrodynamics and water quality a role in controlling the success of fertilization, the food web of fish larvae, and the life cycle of fish larvae. Eggs and larvae are planktonic in the water column, and current patterns determine their distribution. Fish resources are sustainable, If currents spread them into good quality waters, and if not, fish deaths occur prematurely.

AUTHORS CONTRIBUTIONS

Suhaemi performed the conception and design, ran the model, conducted field sampling, analyzed and interpreted the data, and drafted the original manuscript. D.G. Bengen performed the conception and design, critical revision of the manuscript, and supervision. C.P.H. Simanjuntak performed a critical revision of the manuscript and supervision. A.F. Koropitan performed the conception and design, running the model, critical revision of the manuscript, and supervision.

ACKNOWLEDGEMENT

CONFLICT OF INTEREST

OPEN ACCESS

PUBLISHER'S NOTE

ABBREVIATIONS

ADCP	Acoustic doppler current profiler, current recorder
CTD	Conductivity temperature-depth
cm/s	Centimeters per second
DHI	Danish hydraulic institute
dz	Differential to depth
d	depth
ECMWF	European center for medium-range weather forecasts
Eq	Equation
f	Coriolis force
F_u, F_v	Gradient friction horizontal component in x- and y-axis
Fig	Figure
g	Gravitational acceleration
GMT	Greenwich mean time
h	Total depth
Ha	Hectares
IIE	Institute of International Education
ITF	Indonesian throughflow
kg/m^3	Kilogram per cubic meter
Km	Kilometers
K1	Constituents main luni-solar diurnal
Km^2	Square kilometers
K	Turbulence energy kinetic per unit mass
m/s	Meters per second
m	Meter
m^2/s	Square meters per second
M2	Constituents main lunar semi-diurnal
MLD	Mixed layer depth
O1	Constituents main lunar diurnal
Pa	Pascal, atmospheric pressure
PSU	Practical salinity units
S2	Constituents main solar semi-diurnal
S	Source
SPAGs	Spawning aggregation site
Sxx, Sxy, Syx, Syy	Tensor stress radiation component in x- and y-axis
t	Time
T_{pot}-S	Potential temperature-salinity
USAID	The united states agency for international development
u, v, w	Velocity component in x-, y-, and z-axis
u_s, v_s	Sources of velocity component in x- and y-axis
vt	Eddy viscosity, turbulence vertical
x, y, z	Axes in coordinate system
<	Less than
>	Greater than

∂	Differntial
∂u/∂t	Acceleration
∂u/∂x	Differential velocity in x-direction
∂v/∂y	Differential velocity in y-direction
∂w/∂z	Differential velocity in z-direction
η	Surface elevation
%	Percent
'	Minute
"	Second
°	Degree
°C	Degree celcius
°S	Degree south
°N	Degree north
°E	Degree east
ρ	Density
ρo	Density standard
ε	Kinetic energy dissipation per unit mass
3D	Three dimensional

REFERENCES

Adibhusana, M.N.; Hendrawan, I.G; and Karang, I.W.G.A., (2016). Model hidrodinamika pasang surut di perairan pesisir barat kabupaten Badung, Bali. J. Mar. Aquat. Sci., 2(2): 54-59 (**6 pages**).

Budiman, A.S.; Koropitan, A.F.; Wayan, N.I., (2014). Pemodelan hidrodinamika arus pasang surut Teluk Mayalibit kabupaten Raja Ampat provinsi papua barat. Depik. 3(2): 146-156 (**11 pages**).

Canuto, V.M.; Howard, A.; Cheng, Y.; Dubovikov, M.S., (2001). Ocean turbulence. Part I: One-point closure model-momentum and vertical heat diffusivities. J. Phys. Oceanogr., 31(6): 1413–1426 (**14 pages**).

Colberg, F.; Brassington, G.B.; Sandery, P.; Sakov, P.; Aijaz, S., (2020). High and medium resolution ocean models for the Great Barrier Reef. Ocean Model., 145: 101507 (**25 pages**).

Cook, S.E.; Lippmann, T.C.; Irish, J.D., (2019). Modeling non-linear tidal evolution in an energetic estuary. Ocean Model., 136: 13–27 (**15 pages**).

Ferrarin, C.; Bellafiore, D.; Sannino, G.; Bajo, M.; Umgiesser, G., (2018). Tidal dynamics in the inter-connected Mediterranean, Marmara, Black and Azov seas. Prog. Oceanogr., 161: 102–115 (**14 pages**).

George, G.; Desai, D.V.; Gaonkar, C.A.; Aboobacker, V.M.; Vethamony, P.; Anil, A.C., (2013). Barnacle larval transport in the Mandovi-Zuari estuarine system, central west coast of India. J. Oceanogr., 69(4): 451–466 (**16 pages**).

Hadikusumah, (2010). Massa air subtropical Di Perairan Halmahera. J. Ilm. Tek. Kel. Trop., 2(2): 92–108 (**17 pages**).

Haditiar, Y.; Putri, M.R.; Ismail, N.; Muchlisin, Z.A.; Ikhwan, M.;

Rizal, S., (2020). Numerical study of tides in the Malacca Strait with a 3-D model. Heliyon. 6(9): e04828 (**16 pages**).

Hutabarat, M.F.; Purba, N.P.; Astuty, S.; Syamsuddin, M.L.; Kuswardani, A.R.T.D., (2018). Variabilitas lapisan termoklin terhadap kenaikan mixed layer depth (MLD) di Selat Makassar. J. Perikan. Kelaut. 9(1): 9–21 (**13 pages**).

Hendrawan, G.; Nuarsa, I. W.; Sandi, W.; Koropitan, A. F.; Sugimori, Y., (2005). Numerical Calculation for the Residual Tidal Current in Benoa Bay-Bali Island. Int. J. Remote Sens. Earth Sci., 2, 86-93 (**8 pages**).

Ilahude, A.G.; Gordon, A.L., (1996). Thermocline stratification within the Indonesian seas. J. Geophys. Res., 101(C5): 12401–12409 (**9 pages**).

Ivanov, E.; Capet, A.; Barth, A.; Delhez, E.J.M.; Soetaert, K.; Grégoire, M., (2020). Hydrodynamic variability in the southern bight of the North Sea in response to typical atmospheric and tidal regimes. Benefit of using a high resolution model. Ocean Model., 154: 101682 (**15 pages**).

Izquierdo, A.; Mikolajewicz, U., (2019). The role of tides in the spreading of Mediterranean outflow waters along the southwestern Iberian margin. Ocean Model., 133: 27–43 (**17 pages**).

Koropitan, A.F.; Hadi, S.; Radjawane, I., (2006). Three-Dimensional Simulation of Tidal Current in Lampung Bay: Diagnostic Numerical Experiments. Int. J. Remote Sens. Earth Sci., 3: 41-50 (**10 pages**).

Koropitan, A.F.; Barus, T.A.; Cordova, M.R., (2021). Coastal Water Properties and Hydrodynamic Processes in the Malacca Strait: Case Study Northeastern Coast of Sumatra, Indonesia. J. Ecol. Eng., 22(11): 16–29 (**14 pages**).

Lee Sang-Ho.; Beardsley, R., (1999). Influence of stratification on residual tidal current in the Yellow Sea. J. Geophys. Res., 104(7): 15,679-15,701 (**23 pages**).

Noya, Y. A.; Purba, M.; Koropitan, A. F.; Prartono, T., (2016) Cohesive sediment transport modeling on inner Ambon Bay. J. Ilmu dan Teknol. Kelaut. Tropis, 8(2): 671–687 (**18 pages**).

Noya, Y. A.; Kalay, D.E.; Purba, M.; Koropitan, A. F.; Prartono, T., (2021). Modelling baroclinic circulation and particle tracking in inner Ambon Bay. IOP Conf. Series. Earth Environ. Sci., 339: 1-13 (**13 pages**).

Porter, M.; Dale, A.C.; Jones, S.; Siemering, B.; Inall, M.E., (2018). Cross-slope flow in the Atlantic Inflow Current driven by the on-shelf deflection of a slope current. Deep Sea Res. Part I., 140: 173–185 (**13 pages**).

Pradhan, U.K.; Mishra, P.; Mohanty, P.K.; Panda, U.S.; Ramanamurthy, M.V., (2020). Modeling of tidal circulation and sediment transport near tropical estuary, east coast of India. Reg. Stud. Mar. Sci., 37: 101351 (**13 pages**).

Pringle, W.J.; Wirasaet, D.; Suhardjo, A.; Meixner, J.; Westerink, J.J.; Kennedy, A.B.; Nong, S., (2018). Finite-element barotropic model for the Indian and western Pacific oceans: Tidal model-data comparisons and sensitivities. Ocean Model., 129: 13–38 (**26 pages**).

Purba, G.Y., (2020). Water temperature increasing caused mastigias Papua disappeared in marine lake lenmakana Misool Raja Ampat regency, West Papua. J. Sumb. Akua. Indopas., 4(1): 1-10 (**10 pages**).

Quaresma, L.S.; Pichon, A., (2013). Modelling the barotropic tide along the West-Iberian margin. J. Mar. Syst., 109–110: S3–S25

(**23 pages**).

Radjawane, I.M.; Hadipoetranto, P.P., (2014). Karakteristik Massa Air di Percabangan Arus Lintas Indonesia Perairan Sangihe Talaud Menggunakan Data Index Satal 2010. J. Ilm. Tek. Kelaut. Trop., 6(2): 525–536 (**12 pages**).

Rijn, L.C., (2011). Analytical and numerical analysis of tides and salinities in estuaries; Part I: Tidal wave propagation in convergent estuaries. Ocean Dyn., 61(11): 1719–1741 (**23 pages**).

Sabhan; Labania, H.M.D.; Mudin, Y.; Rahman, A., (2021). Modeling of tidal current and residual currents patterns in Tomori Bay, North Morowali regency, Central Sulawesi province. J. Phys. Conf. Ser., 1763: 012025 (**8 pages**).

Sabhan.; Koropitan, A.F.; Purba, M.; Widodo Setiyo Pranowo, W.S., (2019). 3D Simulation Model of Tidal, Internal Mixing and Turbulent Kinetic Energy of Palu Bay. Nat. Environ. Pollut. Technol., 18 (4): 1083-1094 (**12 pages**).

Sala, R., (2018). Model pengelolaan perikanan tangkap berkelanjutan pada zona pemanfaatan tradisional di perairan selatan Pulau Misool, Raja Ampat. Dissertation. IPB University.

Sala, R.; Marsaoly, D.; Dasmasela, H.Y.; Parenden, D.; Orisu, D.; Tarigan, R.B., (2020). Ecological status of target fishes inside and outside marine conservation area of Batbitim, Misool, Raja Ampat. IOP Conference Series. Earth Environ. Sci.,. 429 012054

(**9 pages**).

Sawairnathan, M.; Halimoon, N., (2017). Assessment of the local communities' knowledge on mangrove ecology. International Journal of Human Capital in Urban Management 2(2): 125-138 (**14 pages**).

Seiler, L.; Figueira, R.C.L.; Schettini, C.A.F.; Siegle, E., (2020). Three-dimensional hydrodynamic modeling of the Santos-São Vicente-Bertioga estuarine system, Brazil. Reg. Stud. Mar., Sci., 37: 101348 (**14 pages**).

Sorourian, S.; Huang, H.; Li C.; Justic, D.; Payandeh, A.R., (2020). Wave dynamics near Barataria Bay tidal inlets during spring–summertime. Ocean Model., 147: 101553 (**22 pages**).

Smagorinsky, J., (1963). General circulation experiments with the primitive equations: I. The basic experiment. Mon. Weather Rev., 91(3): 99-164 (**66 pages**).

Thomson, R. E.; Emery, W.J., (2014). Data analysis methods in physical oceanography. Newnes.

Werner, F.E.; Cowen, R.K.; Paris, C.B., (2007). Coupled biological and physical models: Present capabilities and necessary developments for future studies of population connectivity. Oceanography. 20(3): 54–69 (**16 pages**).

Zhang, F.; Sun, J.; Lin, B.; Huang, G., (2018). Seasonal hydrodynamic interactions between tidal waves and river flows in the Yangtze Estuary. J. Mar Syst., 186: 17–28 (**12 pages**).

AUTHOR (S) BIOSKETCHES

Suhaemi, Ph.D. Candidate, Assistant Professor, Department of Marine Sciences, Faculty of Fisheries and Marine Science, University of Papua, Manokwari 98314, Indonesia.
- Email: *s.manaf@unipa.ac.id*
- ORCID: **0000-0003-4585-2277**
- Web of Science ResearcherID: AAD-3228-2022
- Scopus Author ID: 57215859670
- Homepage: https://fpik.unipa.ac.id/pendidikan/jurusan-ilmu-kelautan/

Bengen, D.G., Ph.D., Professor**,** Department of Marine Sciences and Technology, Faculty of Fisheries and Marine Science, IPB University, Bogor 16680, Indonesia.
- Email: *dieter@indo.net.id*
- ORCID: **0000-0002-3880-5117**
- Web of Science ResearcherID: NA
- Scopus Author ID: 55845650900
- Homepage: http://itk.ipb.ac.id/~itkipb/prof-dr-ir-dietriech-g-bengen-dea/

Simanjuntak, C.P.H., Ph.D., Associate Professor, Department of Aquatic Resources Management, Faculty of Fisheries and Marine Science, IPB University, Bogor 16680, Indonesia.
- Email: *charles_phs@apps.ipb.ac.id*
- ORCID: **0000-0002-7673-0435**
- Web of Science ResearcherID: AAD-3210-2022
- Scopus Author ID: 56426082600
- Homepage: http://msp.fpik.ipb.ac.id/en/charles-p-h-simanjuntak/

Koropitan, A.F., Ph.D., Associate Professor, Department of Marine Sciences and Technology, Faculty of Fisheries and Marine Science, IPB University, Bogor 16680, Indonesia.
- Email: *alan@apps.ipb.ac.id*
- ORCID: **0000-0001-5794-094X**
- Web of Science ResearcherID: ABE-7099-2021
- Scopus Author ID: 23135214600
- Homepage: https://itk.ipb.ac.id/~itkipb/dr-alan-frendy-koropitan-s-pi-m-si/